Carrier-Mediated Transport Can Obey Fractal Kinetics

Panos Macheras[1]

Received August 16, 1994; accepted November 8, 1994

A model based on the fractal methodology is proposed for the kinetic study of carrier-mediated transport under heterogeneous conditions, i.e., when the drug-carrier interaction occurs at an interface with an effective dimensionality smaller than the embedding dimension of d = 2. A model equation is derived for the flux, based on a similar approach for an analogous equation for enzyme kinetics. It is shown that the total flux-solute concentration plots are curvilinear when the fractal dimension is smaller than unity while they become biexponential, with ascending and descending limbs, when the fractal dimension D is in the range $1 < D < 2$. Nonlinear Lineweaver-Burk plots are obtained when this fractal kinetics approach is used. Good fittings are obtained when the fractal model is applied to literature data previously analysed with a combined transport mechanism, revealing experimental systems that display a D value in the range $1 < D < 2$. It is suggested that transport studies should be carried out at a wider working solute concentration range and various agitation and incubation conditions in order to derive definite conclusions for the transport pathways.

KEY WORDS: carrier-mediated transport; fractal kinetics; fractal dimension.

INTRODUCTION

Characterizing the permeation of drugs across biological membranes has been of considerable interest in recent years (1). Three classes of methods, namely, *in vitro, in situ* and *in vivo* have been developed to study the basic mechanisms of membrane transport in animals. *In vitro* and *in situ* techniques are indispensable to give information on the kinetic and mechanistic aspects of membrane transport which cannot be gained *in vivo*.

Solutes cross the epithelial membranes by three distinct mechanisms: passive diffusion (paracellular or transcellular), pinocytosis, and carrier mediated transport. Passive diffusion refers to the movement of a solute along its concentration gradient while carrier mediated transport is made possible by membrane proteins reversibly binding specific substrates.

Carrier mediated transport of drugs occurs in various tissues in the body such as kidneys (tubular secretion), mucosal cells in the gut (intestinal absorption and secretion), liver (hepatobiliary excretion) and choroid plexus (removal of drug from the cerebrospinal fluid).

Up to now, the analysis of carrier mediated transport relies on classical reaction kinetics where the rate constants do not have any time dependence. However, this type of kinetics has been found to be unsatisfactory for heterogeneous reactions when the reactants are spatially constrained on the microscopic level by either walls, phase boundaries or force fields (2). Thus, fractal reaction kinetics has been developed for the interpretation of results of experiments with dimensional constraints (3). Fractal like reaction kinetics is particularly suitable for reactions in or on media with inefficient stirring conditions confined to low dimensions, because stirring breaks up the density fluctuations that are generated in such low-dimensional systems rendering the system back to the classical behavior.

Conceptually, the interaction of drug with carrier, which takes place at the interface of different phases, can be considered heterogeneous and spatially constrained because of the restricted movement of the carrier on the complex biological membrane. In addition to this, the "unstirred water layer" in the microenvironment of the gastrointestinal membrane in conjunction with the gradation of pH and the dilemma of the "virtual pH" prevailing in this region, contribute to the inherent geometric heterogeneity of the drug-carrier interaction. However, all previous studies dealing with the effect of unstirred water layer resistance on the rate of carrier mediated transport have been based on classical kinetics (4–6). Accordingly, this study was undertaken to draw attention and apply the fractal kinetics methodology to the analysis of carrier-mediated transport data.

THEORY

Equation 1 is used for the analysis of data in all studies where a carrier mediated transport mechanism is assumed

$$J = J_{max}C/(K_m + C) \quad (1)$$

where J represents the total flux, J_{max} the maximum carrier flux, K_m is the Michaelis constant corresponding to the concentration required for half-maximal transport, and C the solute concentration in the donor compartment. Equation 1 relies on the well-known Michaelis-Menten equation

$$v = V_{max}C/(K_m + C) \quad (2)$$

where v is the reaction rate, V_{max} is the maximum reaction rate, K_m is the Michaelis constant, and C the solute concentration for the enzyme catalysed reaction:

$$E + S \underset{k_{-1}}{\overset{k_1}{\rightleftharpoons}} ES \xrightarrow{k_2} \text{Products} \quad (3)$$

where E is the enzyme, S is the substrate, and k_1, k_{-1}, and k_2 are rate coefficients.

Fractal Kinetics in Enzyme Catalysis and Drug-Carrier Interaction

Based on the principle of fractal dimension and the concepts of fractal kinetics developed by Mandelbrot (7) and Kopelman (3), Quintela and Casado (8) introduced a modified Michaelis-Menten equation for the kinetic study of enzyme catalysis:

$$v = V_{max}^{eff}(C)^{2-D}/(K_m^{eff} + C) \quad (4)$$

where D is a dimensionless number, the fractal dimension,

[1] Laboratory of Biopharmaceutics and Pharmacokinetics, Department of Pharmacy, University of Athens, Panepistimiopolis, Athens 15771, Greece.

0724-8741/95/0400-0541$07.50/0

while V_{max}^{eff} and K_m^{eff} are defined in terms of the time-dependent effective individual rate constants k_i^{eff} for the formation and decomposition of the enzyme-substrate intermediate:

$$E + S \underset{k_{-1}^{eff}}{\overset{k_1^{eff}}{\rightleftharpoons}} ES \xrightarrow{k_2^{eff}} \text{Products} \qquad (5)$$

For D = 1, Equation 4 collapses to the classical Equation 2.

Building on the work of Kopelman (2,3) and Quintela and Casado (8), considering the drug molecules as random walkers and the carrier enzyme as "sitters" (traps), Figure 1, the effective rate coefficients $(k_i^{eff})_{car}$ of the formation and decomposition of the drug-carrier complex

$$\text{Drug}_{(\text{outside cell})} + \text{Carrier} \underset{(k_{-1}^{eff})_{car}}{\overset{(k_1^{eff})_{car}}{\rightleftharpoons}} (\text{Drug-Carrier})_{complex} \xrightarrow{(k_2^{eff})_{car}} \text{Drug}_{(\text{inside cell})} \qquad (6)$$

can be considered proportional to the "efficiency", dG/dt, of the drug (walker):

$$(k^{eff})_{car} \sim dG/dt \qquad (7)$$

where $G(t)$ is a microscopic quantity corresponding to the exploration space of the distinct carrier molecules visited by the drug, Figure 1. However, the quantity G is a function of time (2):

$$G = G(t) \qquad (8)$$

From Equations 7 and 8 it can be concluded that the effective rate constants are time-dependent coefficients. Specifically, it has been shown (2) that for locally heterogeneous media

$$G \sim t^{d_s/2} \qquad (9)$$

where d_s is the "spectral dimension" which is related to the probability of the random walker (drug) to return to its origin after time t (3). As a matter of fact, for all fractal structures $d_s < d$ (topological dimension). From Equation 9 the efficiency, dG/dt, of the drug (walker) can be derived:

$$dG/dt \sim t^{-h} \qquad 0 < h < 1 \qquad (10)$$

where $h = 0$ for $d_s > 2$, and $h = 1 - d_s/2$ for $d_s < 2$. Combining Equations 7 and 10, one has

$$(k^{eff})_{car} \sim t^{-h} \qquad (11)$$

As has been pointed out by Mandelbrot (7) a system is fractally structured if a property or quantity to be measured is, within certain limits, a function of the scale applied. According to Quintela and Casado (8) the "measured" k^{eff} values are dependent on the scale or resolution applied in the enzyme catalysed reaction. This is expressed mathematically with the typical equation of the autosimilarity law (8):

$$k^{eff} = \epsilon^{1-D} \qquad (12)$$

where ϵ is the scale of measurement. Based on the fact that our detailed knowledge (on resolving power) of the enzyme catalysed reaction increases as the working concentration becomes smaller, Equation 12 was expressed in terms of drug concentration (8):

$$k^{eff} = A_i(C)^{1-D} \qquad (13)$$

where A_i is a proportionality constant with the same dimensions used for k^{eff} multiplied by (concentration)$^{D-1}$. Finally, Equation 4 was derived (8) after appropriate combination of Equations 2 and 13.

Applying identical syllogisms to the carrier mediated transport, one can also argue that the resolving power when studying the properties of drug-carrier interaction is also a

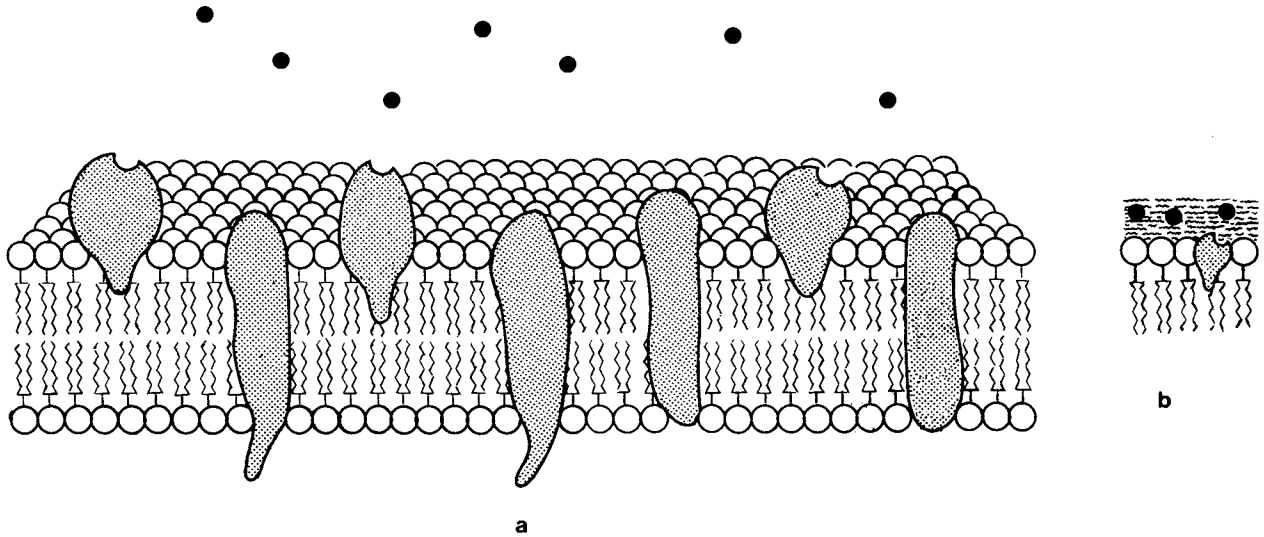

Fig. 1. (a) Schematic representation of the drug-carrier interaction using the fluid mosaic model of a cell membrane. The white circles represent ionic and polar head groups of the phospholipid bilayer, while the wavy lines correspond to the hydrophobic fatty acid chains. Solid bodies with a drug binding site on their surfaces represent the carrier-enzymes (peripheral proteins) attached to the membrane. The solid bodies which traverse the bilayer are integral proteins. The black circles represent the drug. (b) Cross-section of the membrane emphasizing the unstirred water layer overlying the transport sites.

function of the scale applied. For example, if one was able to monitor the energy levels of drug and drug-carrier complex during the movement of drug from the outer to the inner membrane surface, the recorded energy profile for active transport will be dependent on the magnifying capability of the device used for monitoring, Figure 2. In this Figure starting from the unstructured, line (a) the lines b–d show examples with increasing structure. The information contained in these lines can be associated with the intermediate stages of an assumed translocation mechanism of transport, Figure 3. Line (a) of Figure 2 corresponds to the formal Michaelis-Menten kinetics and mirrors the energy levels of the two extreme stages of active transport, designated as 1 and 4, in Figure 3. However, Figure 3 shows only four, among the numerous, stages of the drug transport mechanism across the membrane. Thus, line (a) contains limited information, i.e., the energy difference of the uphill transport of drug. The irregular lines of Figure 2 contain richer information (increasing from b to d) for the energy levels of the intermediate stages of the complex's translocation (designated as 2 and 3) and numerous others not shown in Figure 3. The minima and maxima of the ragged lines (b–d) in Figure 2 correspond to locally stable and unstable configurations of the drug-carrier complex, respectively, during its translocation in the membrane, Figure 3. The equivalence of the curve from one scale to the next in Figure 2 (its self-similarity) is analogous to the self-similarity of the curve in the enzyme catalysed reaction (8). Thus, the "measured" $(k^{\text{eff}})_{\text{car}}$ will be a function of the scale used and the autosimilarity law (Eq. 12) is also applicable here. Plausibly, the lower the concentration used the more accurately one maps the energy profile and in turn measures the $(k^{\text{eff}})_{\text{car}}$ of the carrier mediated transport. Consequently, an analogous equation to Equation 13 can be written:

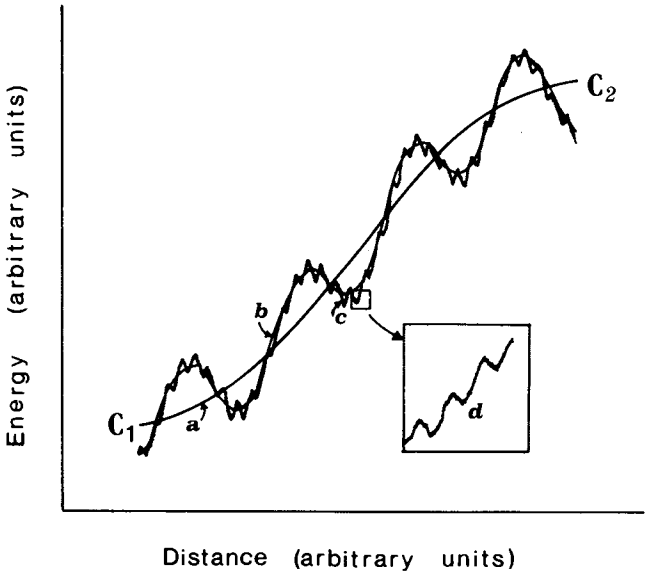

Fig. 2. Schematic representation of the potential energy levels against the distance of the membrane for different resolving power in the active transport mechanism. C_1 and C_2 represent concentrations at the outer and inner membrane surfaces, respectively. See text for the meaning of symbols a, b, c, and d. The inset shows that line d is derived from line c after magnification.

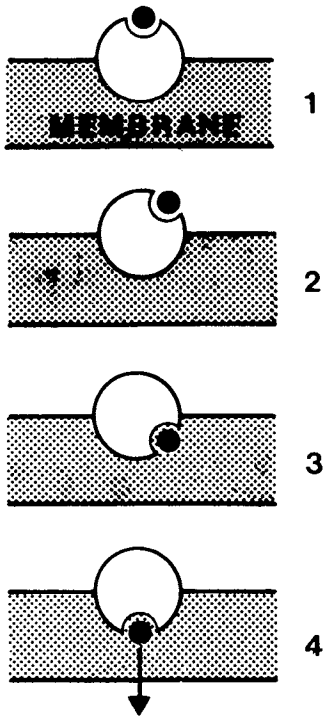

Fig. 3. Schematic representation of drug movement in four steps through membrane following a carrier mediated active transport mechanism. The black circle represents the drug. The coupling energy-yielding process to form or cleave the drug carrier complex is not shown.

$$(k^{\text{eff}})_{\text{car}} = A_i(C)^{1-D} \tag{14}$$

Finally, a modified equation for carrier mediated transport, which takes into account the fractal behavior of the system, can be obtained by combining Equations 1 and 14:

$$J = J_{\max}{}^{\text{eff}} C^{2-D}/(K_{\text{m}}{}^{\text{eff}} + C) \tag{15}$$

where $J_{\max}{}^{\text{eff}}$ and $K_{\text{m}}{}^{\text{eff}}$ are defined in terms of the effective individual rate constants adhering to Equation 6. The similarity of Equation 15 to Equation 4 is obvious, as the two approaches are similar.

Inspection of Equation 15 reveals that for $D = 1$ Equation 15 collapses to Equation 1 and the effective parameters become identical to the conventional Michaelian-type parameters $J_{\max}$ and K_m. This case of $D = 1$ is considered to be the "classical" approach, which assumes a homogeneous embedding space, and homogeneous (well-stirred) reaction conditions. Equation 15 departs from this view by assuming that the dimensional excess of D (i.e., the difference of the exponent value from $D = 1$) is a measure of the degree of the complexity of the mechanism studied.

RESULTS AND DISCUSSION

Figure 4 shows the relation between the total flux and the solute concentration in the donor compartment as a function of different values of the fractal dimension ($0 < D \leq 1$). The deviations from the typical Michaelian curve ($D = 1$) become larger as the values of D become much smaller than the topological dimension, $d = 1$. For this lower fractal dimension ($D < 1$) the total flux increases without reaching a

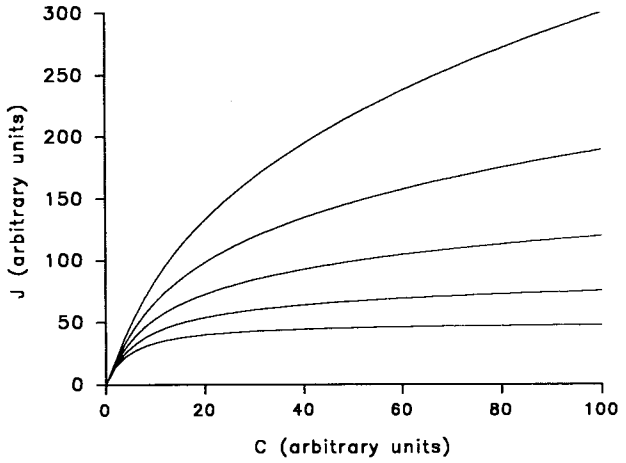

Fig. 4. Theoretical relationship between the kinetics of carrier mediated transport and variations in the fractal dimension D in the range $D \leq 1$ (Eq. 15, using $J_{max}^{eff} = 50$, and $K_m^{eff} = 5$). The values of D from top to bottom are: 0.6, 0.7, 0.8, 0.9, 1.0. Note that each D value corresponds to a different drug-carrier interaction.

plateau value as the solute concentration increases, Figure 4. The curves of Figure 4 are curvilinear-like and approach asymptotically straight lines with slopes which increase as the deviation of D from unity also increases. This kinetic behavior reveals that the mechanism of the reaction (Eq. 6) becomes more complex involving more and more steps (Fig. 3) as the fractal dimension decreases in this low dimensional medium. Therefore, the attainment of a maximum rate of transport is unfeasible, Figure 4.

Figure 5 shows the relation between the total flux and the solute concentration in the donor compartment as a function of different values of the fractal dimension ($1 \leq D < 2$). The overall pattern of these curves demonstrate a unique characteristic since the rate of transport rises at first rapidly, traverses a maximum, and then descends slowly. The deviations from the typical Michaelian curve ($D = 1$) become larger as the values of D become much larger than the topological dimension, $d = 1$. The values of the solute concentration (designated as C_{max}), which correspond to the maxima of the curves in Figure 5, can be calculated by equating with zero the first derivative of Equation 15 and solving the resulting equation:

$$C_{max} = K_m^{eff}(2 - D)/(D - 1) \quad (16)$$

Figure 5 reveals that that the values of C_{max} decrease as the deviation of D from unity increases. The corresponding value for the true total maximum flux, J_{max}^{tot}, can be obtained by combining Equations 15 and 16:

$$J_{max}^{tot} = J_{max}^{eff}(2 - D)^{2-D}[(D - 1)/K_m^{eff}]^{D-1} \quad (17)$$

In the classical reaction system (Figs. 4 and 5, $D = 1$), the steady-state is stable since the rate of arrival of drug inside the cell, (Eq. 6), remains constant due to the random distribution of the walker (drug) in the reaction space. In the fractal-like reaction systems (curves with $D < 1$ in Figure 4 and curves with $1 < D < 2$ in Fig. 5), the distribution of drug in the reaction space is more ordered (3) and the steady-state conditions cannot be either achieved, Figure 4, or maintained Figure 5. In fact, the unattainability, Figure 4, and the instability, Figure 5, of the steady-state conditions become more apparent as the deviation of D from unity increases.

There are several systems reported in the literature (9) that exhibit fractal dimensions in the range $1 < D < 2$, as for example a number of proteins, which are in the range between 1.2 and 1.8, entities not very different from the ones examined in this study. Therefore, the potential carrier surface itself may include fractal-like cavities. This geometric disorder can be important when the drug moves in the fractal-like domains of the transmembrane proteins. It has also been supported (10) that carrier-mediated transport may be achieved by diffusion of drug across tetra-, penta-, and hexameric channels lined by similar transmembrane segments, Figure 1. The surface of the pores in these channels can have fractal structure which could retain high specificity for drug transport. In parallel, the fractal dimension is limited to the range $1 < D < 2$ for the fractal model of ion kinetics (11). According to the authors (11) the fractal model is consistent with the conformational dynamics of the channel proteins. Disregarding the exact mechanism of carrier-mediated transport one can argue that surface morphology irregularities and inefficient stirring conditions could form a reaction medium in which the dynamics taking place would exhibit a fractal dimension less than 2.

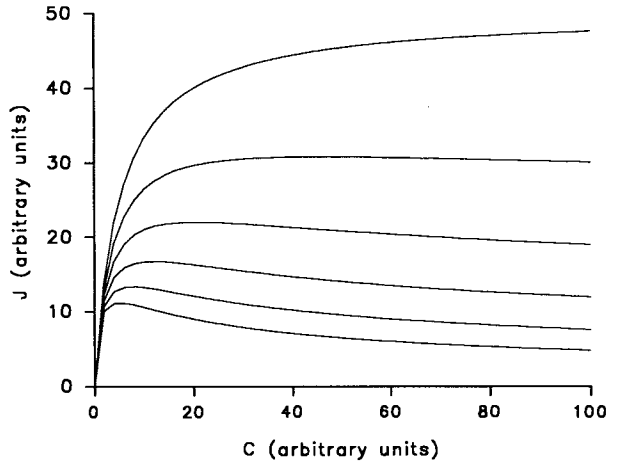

Fig. 5. Theoretical relationship between the kinetics of carrier mediated transport and variations in the fractal dimension D in the range $1 \leq D < 2$ (Eq. 15 using $J_{max}^{eff} = 50$ and $K_m^{eff} = 5$). The values of D from top to bottom are: 1.0, 1.1, 1.2, 1.3, 1.4, 1.5. Note that each D value corresponds to a different drug-carrier interaction.

The Fractal Approach and the Current Analysis of Combined Mechanism

In actual practice non saturable curves similar to those in Figure 4 are commonly encountered in *in vitro* drug transport studies (see for example Ref. 12–14). These curvilinear curves are proposed as evidence in favor of a combined passive and carrier mediated transport mechanism. In all these studies the interpretation of the experimental results relies on the general expression of combined carrier-mediated and passive membrane transport of solutes (12–14):

$$J = [J_{max}C/(K_m + C)] + P_mC \quad (18)$$

where P_m is the passive membrane permeability constant. In fact, Equation 18 consists of an active (the term in brackets) and a passive component (P_mC). The origin of this kind of analysis goes back to the pioneering work of physiologists who identified and quantified the active transfer electrogenic component from the diffusive component during sugar absorption (15). Nevertheless, this is not the case in drug transport studies where Equation 18 is used whenever the concentration dependence for solute transport is not a linear function of the solute donor compartment concentration and a plateau level for maximum transport is not reached. The plots shown in Figure 4 demonstrate that a carrier mediated transport mechanism can exhibit these features if fractal kinetics is encountered. This observation may also apply for the ascending limbs of the curves in Figure 5.

The failure to show a saturable curve may merely indicate fractal kinetics and not a combined mechanism of active and passive transport. It is highly probable that an unstirred water layer overlying the carrier sites, Figure 1, produces concentration heterogeneity in this region. In such a case the value of the fractal dimension, D, will be dependent on the architecture and the agitation conditions of the different kinds of *in vitro* preparations. It is recommended, therefore, that transport studies be carried out with different rates of stirring to assess the rate of transport as a function of the agitation conditions. Accordingly, concern is arising for those techniques, e.g., Caco-2 cell culture model, and Ussing chamber, where solutions are not stirred or agitated during transport experiments.

Usually, the following criteria are applied to transport studies to verify a carrier-mediated mechanism with or without concurrent passive diffusion, i) the transport of a solute is decreased by the addition of metabolic inhibitors or a structural analogue for the carrier binding site and ii) the temperature dependence in carrier mediated transport is higher than in passive diffusion. If fractal kinetics is operating one should also expect the fulfillment of these criteria. Obviously, the presence of a metabolic inhibitor in active transport, causing a disordering of the energy yielding system, will produce a diminution of the rate of drug transport regardless of the type of kinetics, i.e., classical or fractal. The decrease in the rate of drug transport at a lower temperature and in the presence of a competing analogue should be associated with the reduction of the efficiency (Equation 7) of the drug (walker). At lower temperature, apart from the normally postulated reduction of the supplied energy, the exploration space, $G(t)$, of the distinct carrier molecules visited by the drug will be also reduced as a result of the decrease in the diffusivity of drug molecules. In the case of the competing agent, the drug's exploration space will remain the same but the "successful visits" by the walker (drug) will be reduced since the carrier binding sites are occupied by the competitor. The net result of these effects will be the change in $(k^{eff})_{car}$ values (Eq. 14) and therefore an equation analogous to Equation 15 can be written to describe the rate of transport, J_I, under inhibitory conditions assuming that the fractal dimension of the system remains unaltered:

$$J_I = \alpha J_{max}^{eff} C^{2-D}/(\beta K_m^{eff} + C) \quad (19)$$

where α and β are dimensionless, positive coefficients, denoting the change of the true values for the parameters J_{max}^{eff} and K_m^{eff}, respectively.

In most cases, flux-solute concentration plots in the presence of inhibitor seem to be linear. The classical explanation for this linearity is routinely based on the assumption of elimination of the saturable component of Equation 18. However, Equation 19 can also exhibit linear-like behavior in a low and narrow solute concentration range under the inhibitory conditions since α and β can become much smaller and larger than unity, respectively, Figure 6. Presumably, the slight curvature anticipated on the basis of Equation 19 and exemplified in Figure 6 cannot be identified experimentally at this low level of fluxes and under conditions of experimental error. However, whenever a nonlinear flux-concentration curve in the presence of inhibitor is observed, subtraction of the nonsaturable component is applied (14). This kind of data treatment results in apparently linear Lineweaver-Burk plots which are used for the estimation of the Michaelian parameters in the presence of inhibitor. Consequently, caution should be exercised when nonlinear or apparently linear flux-solute concentration plots in the presence of inhibitors are observed.

Lineweaver-Burk Plots

By plotting the inverse of the flux as a function of the inverse of the solute concentration, a linear graph is obtained when data obeying the Michaelian formalism are used, Figure 7 ($D = 1$). The double reciprocal plot is extensively used for calculating, from the slope and the intercept of the straight line, the parameters J_{max} and K_m of Equation 1. However, this kind of plot is nonlinear for fractal-like drug-carrier interactions. The two typical theoretical examples shown in Figure 7 demonstrate that the curve at the vicinity of the origin of the axes concaves downwards for $D < 1$ and upwards for $1 < D < 2$. The use of this plot can be helpful in identifying the range of fractal dimension of the reaction system.

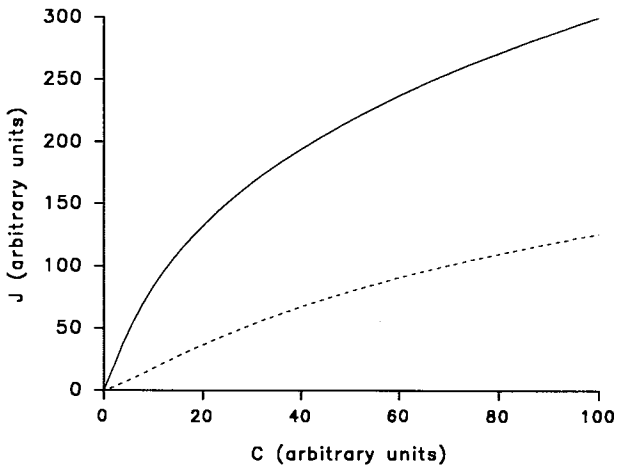

Fig. 6. Simulated curves in the absence (upper curve) and in the presence (lower curve) of inhibitor to demonstrate the apparently linear character of the flux-concentration curve under inhibitory conditions. The upper curve was constructed from $J = 50C^{1.4}/(5 + C)$ while the lower curve from $J = 25C^{1.4}/(25 + C)$.

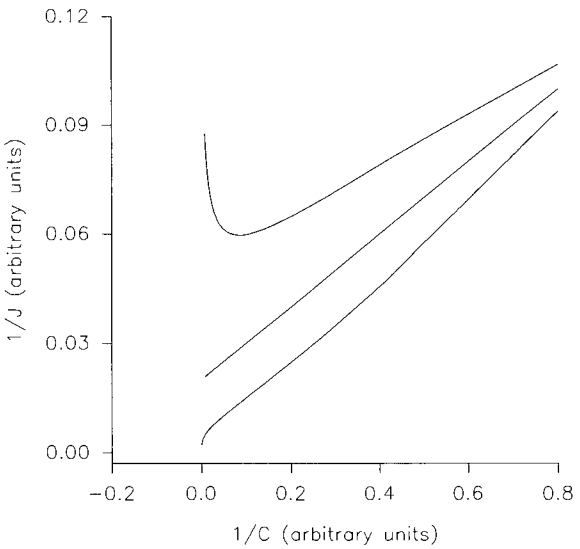

Fig. 7. Lineweaver-Burk plots for D = 1.3 (upper curve), D = 1 (middle curve), and D = 0.7 (lower curve). Equation 15 was used in all cases with J_{max}^{eff} = 50 and K_m^{eff} = 5.

Application of the Fractal Approach to Literature Data

Indications for deviations from the classical Michaelian rectangular hyperbola, mainly due to inefficient stirring, have been previously reported in the literature (4–6). For example, Yuasa *et al.* (6) studied the effect of the unstirred water layer on the Michaelis constant and the maximum transport velocity using a laminar flow model. However, curves resembling those in Figs. 4 and 5 have not been reported since in all studies the analysis was based on the Michaelian formalism, i.e., Equation 2.

Data obtained from the literature for the carrier-mediated transport of arginine (13) and benzoic acid (14) which were previously analysed with Equation 18, are plotted in Figures 8 and 9, respectively, along with the corresponding fitted lines based on Equation 15. The estimates of the parameters for arginine were J_{max}^{eff} = 8.05 (3.52) μmol/hr · cm^2, K_m^{eff} = 31.78 (13.78) mM, D = 1.33 (0.05) and for benzoic acid J_{max}^{eff} = 251.44 (133.31) nmol/min/mg protein, K_m^{eff} = 22.59 (11.03) mM, D = 1.24 (0.09). The square of the correlation coefficients were 0.9996 and 0.9991 for arginine and benzoic acid data, respectively. Figures 8 and 9 demonstrate that fractal kinetics can describe the carrier-mediated transport data of arginine an benzoic acid adequately. The transport rate of benzoic acid under inhibitory conditions (in the presence of 10 mM acetic acid) was also analysed with Equation 15. The experimental data along with the fitted line based on Equation 15 are shown in Figure 10. The value of D was adjusted to 1.24 (estimate found in absence of acetic acid); the estimates of the parameters for the benzoic acid transport in the presence of acetic acid were J_{max}^{eff} = 211.23 (35.15) nmol/min/mg protein K_m^{eff} = 20.88 (5.30) mM, while the square of the correlation coefficient

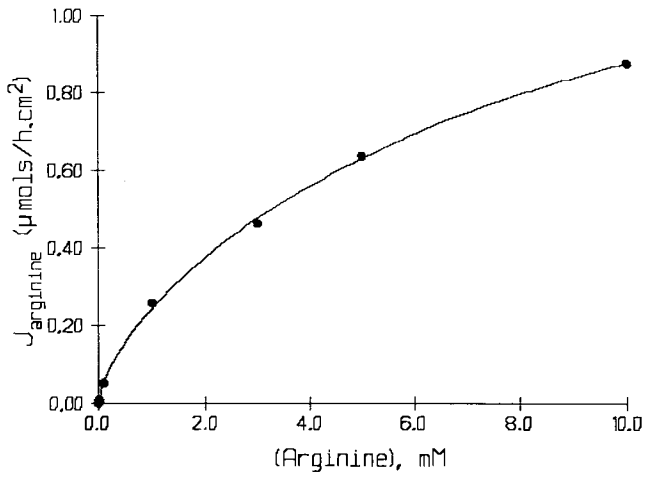

Fig. 8. Concentration dependence of [^{3}H]arginine fluxes in rabbit jejunum taken from Ref. 13. The fitted line based on Equation 15 is also shown.

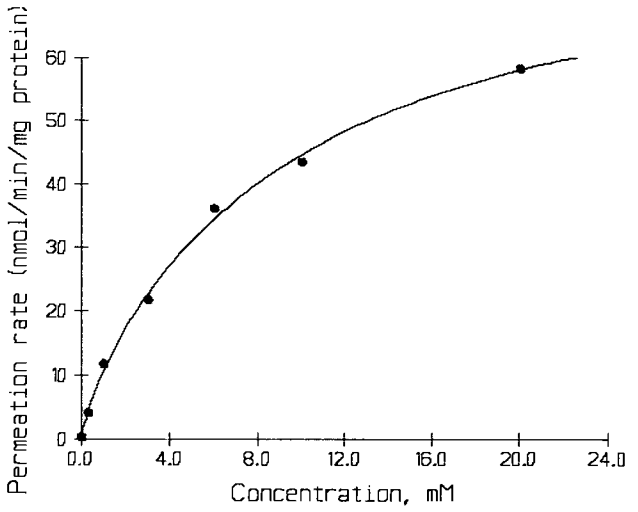

Fig. 9. Concentration dependence of [^{14}C]benzoic acid transport across Caco-2 monolayers at 37°C taken from Ref. 14. The fitted line based on Equation 15 is also shown.

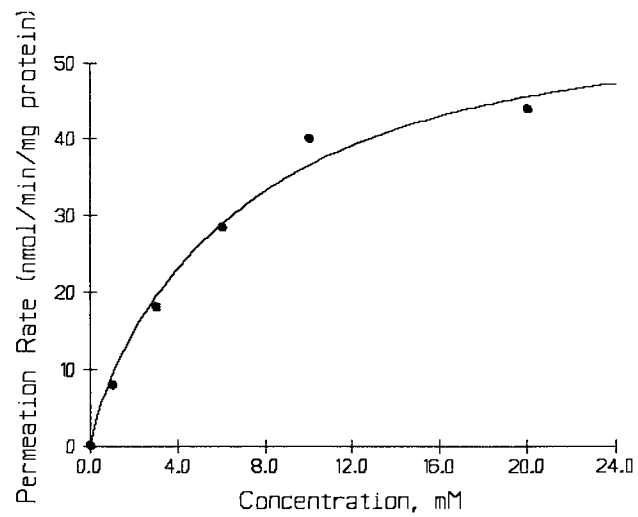

Fig. 10. Concentration dependence of [^{14}C]benzoic acid transport across Caco-2 monolayers in the presence of 10 mM acetic acid at 37°C taken from Ref. 14. The fitted line based on Equation 15 with D = 1.24, is also shown.

was 0.995. Accordingly, the estimates for the parameters α and β of Equation 19 are $\alpha = 211.23/251.44 = 0.84$ and $\beta = 20.88/22.59 = 0.92$.

To the best of my knowledge a total flux-concentration plot, with ascending and descending limbs as depicted in Figure 5 for $1 < D < 2$, has not been previously reported in the literature. According to the current uptake theories, data adhering to the curves of fractal-like kinetics of Figure 5 are "negative" and unexplained and if they have been actually observed they have not been published. However, it is very well known (16) in the field of enzyme kinetics that high concentrations of the substrate are self-inhibitory causing reduction of the rate of the reaction. In addition, Shi *et al.* (17) observed that biotin uptake by bovine brain microvessel endothelial cell monolayers was reduced when concentrations higher than 1000 μM were used. It was also noted in the same article (17) that nonanoic acid and pantothenic acid were significant inhibitors of biotin uptake, but only consistently at longer incubation times. The time dependence of inhibition is not in accord with classical kinetics but is compatible with fractal-like kinetics. Consequently, carrier-mediated transport studies should be carried out using a variety of incubation times in order to evaluate the parameter estimates as a function of time. According to Kopelman (2,3), a log-log plot of the parameter estimates versus time gives a straight line with zero or negative slope when classical or fractal kinetics prevail, respectively.

CONCLUSIONS

In this study, the previous work of Quintela and Casado (8) was extended from the reaction rate of an enzyme-substrate system to the flow of a carrier-mediated drug through a membrane. The same notions were used to set up an equation with characteristic scaling behavior, relating the drug flow to the solute concentration in the donor compartment raised to a power $(2 - D)$, where D is the "fractal" dimension of the process involved. This formalism was subsequently applied to two well known systems, arginine and benzoic acid, and showed a satisfactory fitting of the permeation rate. The present data, which in the past were analyzed with sophisticated but, nevertheless, classical approaches, show that the new fractal approach could also be a plausible valid mechanism, with a value of the D exponent in the range $1 < D < 2$. The approach developed provides a new picture to understand carrier-mediated transport kinetics. Contrary to previous reports (4–6), in the present study inefficient stirring is not expressed explicitly in a mathematical form; here, the approach developed allows all causes (and certainly inefficient stirring is one of them) of fractal kinetics to be studied globally relying on Equation 15. The findings of the present study reveal that if a fractal picture is valid, the effect of temperature and inhibitors on transport rates provide only indications of transport mechanisms. Other experimental manipulations such as, stirring or agitation conditions, a wider working solute concentration range, and various incubation times should be used for detailed determination of transport pathways.

It should be mentioned that fractal kinetics for carrier-mediated transport can also operate under *in vivo* conditions. Depending on the specific characteristics of the system under study and the hydrodynamics prevailing in the reaction space, fractal or Euclidean dimensions can be found in the different regions of the body. For example, the agitation of the water layer adjacent to the gastrointestinal membrane is considered to be less (4) than in *in vitro* preparations. Concern is arising therefore for the utility of the estimates of the parameters J_{max} and K_m derived from Equations 1, 15, and 18 in *in vitro* experiments. In other words, the validity of the *in vitro* parameter estimates of the carrier-mediated transport is questionable when applied to *in vivo* conditions.

Finally, recent work (7,18) has demonstrated that anatomical structures such as the circulatory system and the lungs, may display fractal geometry. In parallel, time-dependent processes exhibiting limit cycle oscillation have been considered responsible for nonlinearity in pharmacokinetics (19). Consequently, the analysis of time-dependent processes operating in a fractal surrounding in the body may require the application of nonlinear dynamics (20). The rich dynamical phenomena in the time course of drug in the body and pharmacodynamics can be better understood using techniques being developed to understand dynamics in nonlinear systems.

ACKNOWLEDGMENTS

The author is indebted to Dr. P. Argyrakis, Department of Physics, University of Thessaloniki, who critically read the manuscript and helped elucidate the concept of the "fractal" dimension as it is applied in the present work. The author would also like to thank Dr. Valsami for her assistance in the computing work and Dr. Swaan, Department of Pharmaceutics, University of Utrecht and Dr. Tsuji, Department of Pharmaceutics, Kanazawa University for providing their data.

REFERENCES

1. G. Wilson. Cell culture techniques for the study of drug transport. *Europ. J. Drug. Metab. Pharmacokin.* 15, 159–163 (1990).
2. R. Kopelman. Rate processes on fractals: theory, simulations, and experiments. *J. Stat. Phys.* 42, 185–200 (1986).
3. R. Kopelman. Fractal reaction kinetics. *Science* 241, 1620–1626 (1988).
4. A.B.R. Thomson, and J.M. Dietschy. Derivation of the equations that describe the effects of unstirred water layers on the kinetic parameters of active transport processes in the intestine. *J. Theor. Biol.* 64, 277–294 (1977).
5. A.B.R. Thomson. Experimental diabetes and intestinal barriers to absorption. *Am. J. Physiol.* 244, G151–G159 (1983).
6. H. Yuasa, Y. Miyamoto, T. Iga, and M. Hanano. Intestinal absorption by carrier-mediated transports: two dimensional laminar flow model. *J. Theor. Biol.* 119, 25–36 (1986).
7. B.B. Mandelbrot. *The Fractal Geometry of Nature* (Freeman, San Francisco, 1983).
8. M.A. Lopez-Quintela, and J. Casado. Revision of the methodology in enzyme kinetics: a fractal approach. *J. Theor. Biol.* 139, 129–139 (1989).
9. H.P. Koch. The concept of fractals in the pharmaceutical sciences. *Pharmazie.* 48, 643–659 (1993).
10. J.B.C. Findlay. The disposition and organization of proteins. In A.J. Turner (eds), *Molecular and Cell Biology of Membrane Proteins* Ellis Horwood Ltd, Southampton, 1990, pp 1–30.
11. L.S. Liebovitch, J. Fischbarg, J.P. Koniarek, I. Todorova, and

M. Wang. Fractal model of ion-channel kinetics. *Biochimica and Biophysica Acta* 896, 173–180 (1987).
12. P.F. Bai, P. Subramanian, H.I. Mosberg, and G.L. Amidon. Structural requirements for the intestinal mucosal-cell peptide transporter: the need for N-terminal α-amino group. *Pharm. Res.* 8, 593–599 (1991).
13. P.W. Swaan, G.J. Marks, F.M. Ryan and P.L. Smith. Determination of transport rates for arginine and acetaminophen in rabbit intestinal tissues *in vitro*. *Pharm. Res.* 11, 283–287 (1994).
14. A. Tsuji, H. Takanaga, I. Tamai, and T. Terasaki. Transcellular transport of benzoic acid across caco-2 cells by a pH-dependent and carrier mediated transport mechanism. *Pharm. Res.* 11, 30–37 (1994).
15. E.S. Debnam, and R.J. Levin. An experimental method of identifying and quantifying the active transfern electrogenic component from the diffusive component during sugar absorption measured *in vivo*. *J. Physiol.* 246, 181–196 (1975).
16. F.B. Armstrong. *Biochemistry,* Oxford University Press, Third Ed., New York, 1989, p. 128.
17. F. Shi, C. Bailey, A.W. Malick, and K.L. Audus. Biotin uptake and transport across brain microvessel endothelial cell monolayers. *Pharm. Res.* 10, 282–288 (1993).
18. B.J. West, and A.L. Goldberger. Physiology in fractal dimensions. *Am. Scientist,* 75, 354–365 (1987).
19. *Chronopharmacology—Cellular and Biochemical Interactions.* Ed. B. Lemmer, Marcel Dekker, New York, 1989.
20. L. Glass, M.C. Mackey. *From Clocks to Chaos—The Rhythms of Life,* Princeton University Press, New Jersey, 1988.